Chemical Engineering Research and Design 215 (2025) 108–121

Contents lists available at ScienceDirect

Chemical Engineering Research and Design

journal homepage: www.elsevier.com/locate/cherd

Optimised model microcapsules of Arabic gum and gelatin a for functional cosmetic applications: From formulation to scale-up using a mesostructured reactor

Júlia C. Kessler [a,b,c,*], Isabel M. Martins [a,b], Yaidelin A. Manrique [a,b], José Carlos B. Lopes [a,b], Alírio E. Rodrigues [a,b], Maria Filomena Barreiro [c,**], Madalena M. Dias [a,b]

[a] LSRE-LCM - Laboratory of Separation and Reaction Engineering - Laboratory of Catalysis and Materials, Faculdade de Engenharia, Universidade do Porto, Rua Dr. Roberto Frias, Porto 4200-465, Portugal
[b] ALiCE - Associate Laboratory in Chemical Engineering Faculdade de Engenharia, Universidade do Porto, Rua Dr. Roberto Frias, Porto 4200-465, Portugal
[c] CIMO, LA SusTEC, Instituto Politécnico de Bragança, Campus de Santa Apolónia, 5300-253 Bragança, Portugal

ARTICLE INFO

Keywords:
Encapsulation
Complex coacervation
Arabic gum+gelatine
Batch mode optimisation
Continuous mode scale-up
NETmix

ABSTRACT

Microcapsules were developed using Arabic gum and gelatin A through complex coacervation, employing both batch and continuous production methods. Ingredients were chosen to encapsulate diverse hydrophobic core materials with functional properties tailored for cosmetic applications, such as those found in commercial hydrating creams, aiming to enhance their performance through microencapsulation. The formulation was optimised by systematically adjusting key parameters to balance the electrostatic and structural behaviour of the polymers, ensuring ideal encapsulation conditions. The optimised batch formulation (3.5:1 vol-to-volume ratio of core material to emulsifier, stirring at 9500 rpm for 2 min, and 10 % crosslinker concentration) resulted in spherical, multinuclear microcapsules with an average size of circa 60 μm, maintaining structural stability over 45 days. Encapsulation efficiency, defined as the percentage of core material successfully enclosed within the microcapsules relative to the initial amount used, reached up to 89 %. Transitioning to a continuous production method using the NETmix reactor further improved performance, achieving an encapsulation efficiency of 98 %. This was accomplished by performing the emulsification and polymer complexation steps under controlled Reynolds numbers of approximately 358 and 559, sustained over 2 and 4 minutes, respectively.

1. Introduction

Microcapsules are delivery systems of compounds protected from environmental stresses within a physical barrier (Butstraen & Salaün, 2014). Core-shell, double-shell, or polynuclear entities are possible morphologies formed due to the interaction between one or more polymers (e.g., protein, polysaccharides), which will surround diverse target compounds in stabilised particles (Butstraen & Salaün, 2014). The wall material, or encapsulating agent, coats the core, also called active material, embedded or not in a carrier (Carvalho et al., 2016).

Microencapsulation by complex coacervation (MCC) is a method used to encapsulate compounds within a protective shell, providing stability to the encapsulated material. This process involves blending two polyelectrolyte solutions with opposite charges, resulting in liquid-liquid phase separation facilitated by interactions such as electrostatic attractions, hydrogen bonding, hydrophobic forces, and polarization-induced effects (Xiao et al., 2014). The process can be summarised in three steps: (i) emulsification of an oil phase in an aqueous solution, (ii) polymer complexation to achieve zero ionic strength, and (iii) formation of a coating network to self-sustain the microparticles (Butstraen & Salaün, 2014; Martins et al., 2014). Each step has distinct effects on particle shape and size distribution, encapsulation efficiency, and stability (Butstraen & Salaün, 2014), highly influenced by the stirring rate, volume ratio of the two phases, and physicochemical properties of the involved polymers (Marfil et al., 2018; Prata & Grosso, 2015). MCC offers multiple advantages in protecting biomolecules, making it

* Corresponding author at: LSRE-LCM - Laboratory of Separation and Reaction Engineering - Laboratory of Catalysis and Materials, Faculdade de Engenharia, Universidade do Porto, Rua Dr. Roberto Frias, Porto 4200-465, Portugal.
** Corresponding author.
E-mail addresses: juliakessler@fe.up.pt (J.C. Kessler), barreiro@ipb.pt (M.F. Barreiro).

https://doi.org/10.1016/j.cherd.2025.01.035
Received 7 September 2024; Received in revised form 12 January 2025; Accepted 24 January 2025
Available online 27 January 2025

increasingly used in industrial settings to develop greener and more sustainable formulations. This technique is often regarded as versatile, economical, and reproducible, with a high encapsulation efficiency (Martins et al., 2014; Muhoza et al., 2020; Timilsena et al., 2019).

Various coacervate systems have been proposed to address challenges related to thermal degradation and the controlled release of functional compounds (Ang et al., 2019; Carpentier et al., 2022; Comunian et al., 2013; Martins et al., 2011b). Some examples of polymeric combinations include Arabic gum (AG) and chitosan (Sharkawy et al., 2017), tragacanth gum and pea protein (Carpentier et al., 2022), and sodium alginate with gelatine (GE) (Bastos et al., 2020) used to encapsulate vanillin and limonene, α-tocopherol, and black pepper oils, respectively. Among these, the blend of AG and GE is one of the most commonly used systems in MCC due to their abundance, biodegradability, and commercial competitiveness, having been first introduced in the mid-20th century (Li et al., 2013; Timilsena et al., 2019). AG is a heteropolysaccharide with unique emulsification properties and high water solubility. On the other hand, GE is a collagen form with high stabilisation characteristics, high crosslinking ability, and thickening properties (Shaddel et al., 2018). Target phytochemicals such as ascorbic acid (Comunian et al., 2013), anthocyanins (Shaddel et al., 2018), carotenoids (Marfil et al., 2018), allyl isothiocyanate (Zhang et al., 2011), and curcumin (Zuanon et al., 2013) have been successfully encapsulated by AG/GE. These tailored coacervates have the potential to enhance the bioavailability of many ingredients used in cosmetic and personal care products, fulfilling the skincare market that is continuously searching for nourishing and anti-ageing solutions and, more recently, for medical drug-like formulations (Taofiq et al., 2016). For example, research data supports the effectiveness of curcumin microcapsules incorporated into a cream formulation for treating burns and promoting wound healing (Ang et al., 2019).

The scalability of microcapsule production is crucial in competitive settings (Ferreira & Nicoletti, 2021; Tang et al., 2020). Continuous microencapsulation has been introduced using the mesostructured reactor NETmix (Lopes et al., 2005), previously optimised for the production of microcapsules by polycondensation (Moreira et al., 2020), Pickering emulsions (Marques et al., 2024; Ribeiro et al., 2021), and microspheres by solvent evaporation (Moreira et al., 2022). NETmix comprises a network of unit cells, each consisting of one chamber connected to two inlet and two outlet channels arranged at a 45° angle to the flow direction (Supplementary Material 1). The chambers serve as mixing zones, while the channels function as transport pathways. The NETmix technology was designed to operate in laminar flow regime. However, when the Reynolds number exceeds a critical value of circa 150, the flow transitions into a self-sustained, dynamic, and chaotic oscillatory regime (Laranjeira et al., 2009; Laranjeira et al., 2011). This transition significantly enhances system efficiency by inducing strong laminar mixing. Moreover, the repetition of the mixing zone ensures a homogeneous flow distribution of the evolving phases, maximizing the interfacial area between fluids (Fernandes et al. 2023), a critical feature for the formation of emulsions and dispersions (Moreira et al., 2020; Ribeiro et al., 2021).

Given the variety of encapsulating systems, this study aims to study polymers' complexation within a pH range and polymer concentrations, targeting cosmetic applications through non-toxic and low-viscosity products. This context has motivated the development of a model microencapsulation system designed as a versatile system to encapsulate different cosmetic ingredients. Built upon an initial survey and thorough extensive testing, the composition was carefully selected to ensure compatibility with commercial formulations while serving the respective functional purposes. The system AG/GE was chosen because of its favourable physicochemical characteristics, such as low viscosities and colourlessness (Yang et al., 2024), along with its ease of use and cost-effectiveness (Shaddel et al., 2018). These characteristics meet the requirements of the mesostructured reactor, and the method used. Caprylic triglyceride (CAP) was selected as the core material, recognised as an emollient and potential carrier of functional hydrophobic compounds used in cosmetic formulations, such as α-tocopherol and those found in *Moringa oleifera* leaf extract (Kessler et al., 2023) and recently reviewed (Kessler et al., 2024). Polysorbate 80 (P80), an ingredient listed in most cosmetic emulsion-based formulations, and often used for the formation of hydrophobic coacervates (Rabisková & Valásková, 2008), was chosen as the emulsifier, while 1-ethyl-3-(3-dimethyl aminopropyl) carbodiimide (EDC) and N-hydroxy succinimide (NHS) were used as crosslinkers due to their non-toxicity and compatibility with GE (Kuijpers et al., 2000). Furthermore, stirring conditions, emulsifier ratio, and crosslinking percentages underwent a dual optimisation process aimed at guiding the development of cosmetic microcapsules in batch mode. The microcapsules formulation that yielded the best results was subsequently scaled up using a mesostructured reactor, NETmix.

This study was tailored for application in cosmetic products, such as hydrating creams, aiming to enhance their performance through microencapsulation. The formulation was optimised by systematically adjusting key parameters to balance the electrostatic and structural behaviour of the polymers, ensuring ideal encapsulation conditions.

2. Material and methods

2.1. Chemicals

Gelatine A (GE, from porcine skin, 300 g bloom, CAS 9000–70–8), Arabic gum (AG, from Acacia tree, CAS 90000–01–5), N-hydroxy succinimide (NHS, purity ≥ 97 %, CAS 6066–82–6), Polysorbate 80 (P80, HLB 4.3, CAS 9005–65–6), hydrogen chloride (HCl, purity ≥ 37 %, CAS 7647–01–0), sodium sulphate anhydrous (Na_2SO_4, CAS 7757–82–6), Nile red (CAS 7385–67–3), and Nile blue A (purity ≥ 75 %, CAS 3625–57–8) were purchased from Sigma Aldrich (Madrid, Spain). 1-ethyl-3-(3-dimethylaminopropyl) carbodiimide (EDC, purity ≥ 98 %, CAS 25952–53–8) was acquired from Alfa Aesar (Budapest, Hungary). Caprylic triglyceride (CAP, from *Cocos mucifera* oil, batch 14832) was obtained from Plena Natura (Lisbon, Portugal), and *n*-hexane (purity 95 % HPLC, CAS 110–54–3) was bought from VWR (Lisbon, Portugal).

2.2. Polymers characterisation

The chemical association between AG and GE was studied, focusing on the electrostatic interactions that promote complexation and analysing the chemical groups involved in the process.

2.2.1. Zeta potential

Zeta potential measurements were conducted to assess the surface charge of both polymers (AG and GE), their electrostatic stabilization properties, and their individual contributions to the system's overall stability. AG and GE solutions were prepared, and their pH was adjusted using HCl 1 M and Na_2SO_4 1 M to a range from 2 to 9. The zeta potential was measured using a Zetasizer Nano ZS90 (Malvern Panalytical Ltd, Malvern, United Kingdom). Samples of both polymers, individually and mixed, were analysed at 20 °C using a capillary Zeta cell (ref: DS7010). The obtained data allowed for determining the appropriate pH for the coacervate formation of the given mixture and estimating the isoelectric point of GE.

2.2.2. Infrared spectroscopy

FT-IR analyses were performed to evaluate the structural response of the polymers to pH variations and their potential influence on microcapsule stability. Aqueous polymer solutions of AG and GE were prepared across a pH range of 2–9 and then freeze-dried under vacuum at −85 °C for 48 hours (6KBTEL-85, VovirTis, Gardiner, NY, United States) to prevent the interference from water. Subsequently, samples of both polymers, individually and mixed, were analysed by Infrared Spectroscopy using a Spectrum Two FT-IR Spectrometer (PerkinElmer, Waltham, MA, USA), equipped with a LiTaO3 detector, operating within a

wavelength range of 4000–400 cm^{-1} at 20°C.

2.3. Microcapsules production

2.3.1. Production of microcapsules in batch mode

The parameters used for the production of tailored microcapsules have been guided by insights gained from previous works, namely polymer concentration and polymer ratio (Yue et al., 2022), crosslinking agents (Kuijpers et al., 2000), and pH for complexation (da Silva et al., 2015). Additionally, preliminary tests were conducted to evaluate the effects of stirring rate and time, the oil-to-aqueous phase and the crosslinkers ratio.

The process starts with the preparation of the primary reactant solutions. Aqueous solutions of AG at 14.30 g•L^{-1} and GE at 7.14 g•L^{-1} are first homogenised under constant stirring, using a polygon stirring bar (Fisher Scientific, 6 mm diameter, 10 mm length) for a minimum of one hour at 40 ºC. The oil phase (CAP:P80) is prepared by mixing 7.5 g of CAP with P80 for three volume-to-volume ratios (CAP:P80 = 5:1, 3.5:1, and 2:1) and stirring until a homogeneous mixture is obtained, then heated at 40 ºC for thermal compatibility with the aqueous phase.

The microcapsule production process in batch mode is described below in seven steps and schematically represented in Supplementary Material 2.

- Step 1 - Emulsification: An emulsion is obtained by mixing 8.4–10.7 g of the oil phase (CAP:P80) with 50 mL of GE solution for specified time and rotation speed in an Ultra Turrax (IKA Yellowline DI 25, Gravimetra, Lisbon).

  Steps 2–5 are subsequently performed under constant stirring at 400 rpm with a magnetic stirrer (Agimatic-N, J.P. Selecta, Barcelona).
- Step 2 - Polymer addition: The emulsion is transferred to a beaker (tall form, capacity of 150 mL, 95 mm height, 54 mm O.D.), and 50 mL of the GA solution is gradually added dropwise over 4 min. The mixture is then stirred continuously using a polygon stirring bar (Fisher Scientific, 6 mm diameter, 10 mm length) for an additional 6 min period at 40 ºC to stabilise the core size constituted by the oil droplets.
- Step 3 - Coacervation: The pH of the oil droplet dispersion is promptly lowered from 5.4 to 3.9 by adding HCl 1 M (see Section 3.1) and monitored using a pH meter (Hanna, HI 8424, Smithfield, United States).
- Step 4 - Cooling: The resulting microcapsules dispersion is slowly cooled down in an ice batch until reaching 7 ºC over a period of 30 min.
- Step 5 - Hardening: EDC 50 mM and NHS 25 mM are added in equal amounts to proceed with the crosslink of the coacervates for 60 min, resulting in the crosslinked microcapsules.
- Step 6 - Decantation: The crosslinked dispersion is transferred into a decantation funnel to induce phase separation under refrigerated conditions (7 ºC) overnight.
- Step 7 - Washing: The resulting concentrated microcapsules phase is collected from the bottom of the decantation funnel, and any remaining non-reacted reagents are washed out twice using 60 mL of deionized water at 40 ºC.

The final rich-concentrated microcapsule dispersion is stored, preservative-free, in a falcon tube and refrigerated until further analyses.

2.3.2. Production of microcapsules in continuous mode

The mesostructured reactor NETmix was used to transfer microcapsule production from batch to continuous mode. To achieve proper mixing and a homogeneous mixture, the two liquids streams must meet a critical Reynolds number,

$$\mathrm{Re} = \frac{\rho v d_h}{\mu} \quad (1)$$

where ρ is de density (kg•m^{-3}), v is the average velocity in the channels (m•s^{-1}), d_h is the channels' hydraulic diameter (m), and μ is the viscosity (mPa•s). It has been shown that for $Re > 150$, the flow evolves into a self-sustained dynamic and chaotic oscillatory flow regime, inducing strong laminar mixing (Laranjeira et al., 2009; Laranjeira et al., 2011). This occurs due to the geometric characteristics of the NETmix network, and the local hydrodynamic instabilities induced by the immerging jet interactions at the chambers (Matos et al., 2024).

Consequently, NETmix has significant advantages over other emulsification devices since it induces successive repeated and well-localised mixing within the chambers throughout the reactor, promoting easily reproducible emulsification steps. The microNETmix device (Ribeiro et al., 2021) used in this work is constructed from stainless steel and features 25 rows and 8 columns; each cylindrical chamber has a diameter of 3.3 mm, while the prismatic channels present a width of 0.5 mm and a length of 1.8 mm. The network depth is 0.5 mm, resulting in a total volume of approximately 1 mL. This device also features two heat-exchange plates enabling isothermal operation.

Fig. 1 shows a schematic representation of the NETmix set-up to produce microcapsules including two peristaltic pumps (Masterflex Ismatec MCP, Avantor VWR, Pennsylvania, United States), a thermostatic bath, and a magnetic stirrer. The experimental setup can be operated in two different modes. In reaction mode (Fig. 1**a**), two streams (either reactant solutions or emulsions/dispersions formed from the previous steps) are fed into NETmix through alternating inlet channels and the resulting emulsion/dispersion collected through the outlet channels. In recirculation mode (Fig. 1**b**), a single stream is fed into the inlet channels, collected through the outlet channels and recirculated. Since the total volume of solution in recirculation is higher than the NETmix volume, to maintain the emulsions/dispersions in constant stirring, the recirculation steps can be assisted by a magnetic stirrer. For both modes, the flow rate is selected to ensure that the average Reynolds number at the outlet channels exceeds the critical threshold while also preventing any clogging and producing an adequate sample quantity.

The MCC batch production sequence was adapted to continuous mode using NETmix. The first five steps are outlined below, with a schematic representation provided in Supplementary Material 3. Steps 6 and 7 are performed in batch mode.

- Step 1 - Emulsification: The GE solution at 7.14 g•L-1 and the CAP:P80 mixture (volumetric ration of 3.5:1) are fed into the NETmix. The resulting emulsion is then recirculated for a fixed period, while keeping the system at 40 ºC.
- Step 2 - Polymer addition: The AG solution at 14.30 g•L-1 and the previous emulsion are then fed into the NETmix. The produced oil droplet dispersion is then recirculated.
- Step 3 - Coacervation: The coacervation of the oil droplets is performed in batch mode lowering the pH from 5.4 to 4.0 using HCl 1 M.
- Step 4 - Cooling: The microcapsules dispersion is cooled down from 40 ºC to 7 ºC while recirculating for 30 min.
- Step 5 - Hardening: EDC/NHS solution is added to the microcapsule's reactor followed by recirculation for 60 min.

Different configurations for Steps 4 and 5 were tested by using either the magnetic stirrer alone, the NETmix system alone, or a combination of both.

The final microcapsule dispersion is stored in similar conditions as those produced in batch mode.

2.4. Microcapsules characterisation

To tailor the formulation for cosmetic applications, the produced

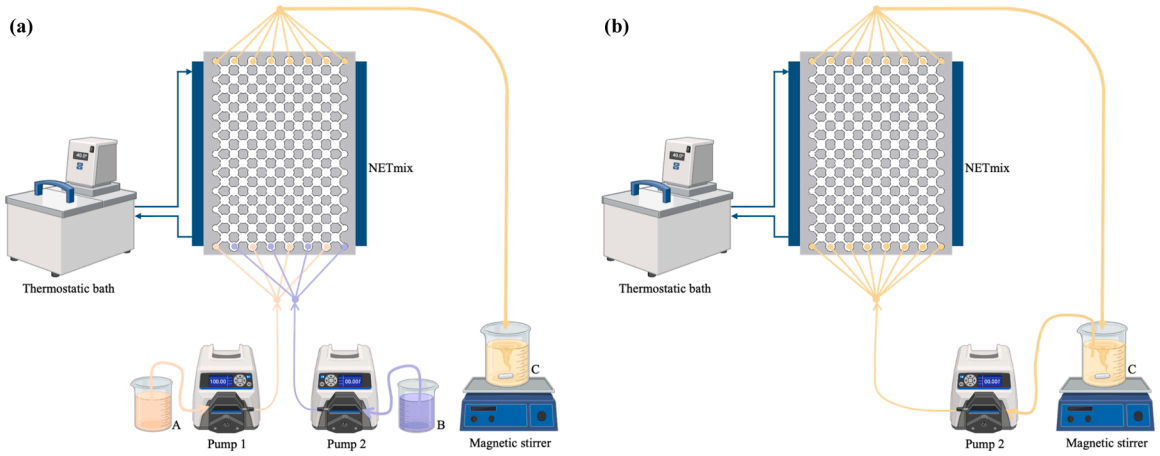

Fig. 1. Schematic representation of the NETmix set-up to produce AG/GE microcapsules: (a) in reaction mode with reactants (A and B) fed into NETmix through two streams to form either emulsions or dispersions (C) collected in the outlet channels; and (b) in recirculation mode with either emulsion or dispersion (C) fed into NETmix through a single stream and collected in the outlet channels.

microcapsules underwent a thorough evaluation, including a series of physicochemical characterisation and imaging analyses. This assessment was designed to evaluate their morphology, structural stability, and microencapsulation efficiency.

2.4.1. Particle size distribution of microcapsules

The particle size distribution of the produced microcapsules was analysed over 30- and 45-day storage periods using a Laser Diffraction Particle Size Analyzer (LS 230, Beckman-Coulter, Brea, CA, United States). Replicate measurements were performed to determine the volume of particles within specific size ranges. The results are presented as the volumetric mean size (D[4,3]), expressed as a percentage, with particle sizes reported in micrometres (μm).

2.4.2. Microcapsules morphology

Microcapsule morphology was analysed by Optical Microscopy (Eclipse Ci H55OS, equipped with camera DS-Qi2, Nikon, Tokyo, Japan) connected to PC NIS-Elements L software. Analyses were performed at magnifications of 10 and 40 times.

The encapsulated oil and produced microcapsules were evaluated by Confocal Laser Scanning Microscopy (DMIB, Leica Microsystems Inc., Heidelberg, Germany) coupled to a white light laser stellaris 8 (440–790 nm) and UV (diode 405 nm/50 mW), equipped with a high-resolution system (8192 ×8192 pixels and 3600 Hz). For this analysis, 0.1 % w/v of Nile red dye was added to the oil phase prior to emulsification, while 0.1 % w/v of Nile blue A was incorporated in the final dispersion. Microcapsule solutions were placed on a concave slide covered with an immersion liquid type F, in which the respective fluorescent dyes were excited by an argon laser at 549 nm and 631 nm, with emissions of 628 nm and 660 nm. The obtained images and videos were processed using IMAGE-J/Fiji (Schneider et al., 2012).

Cryo-Scanning Electron Microscopy (Cryo-SEM, JEOL JSM-6301F, Gatan Alto 2500, Pleasanton, CA, United States) was used to confirm the morphology of the microcapsules. Sample preparation consisted of cryofixation using sub-cooled nitrogen under vacuum, followed by immediate transfer to the pre-chamber where the frozen material was fractured, sublimated at −90 °C for 180 s, and coated with Au/Pd (45 s, 12 mA). The analysis was carried out at −120 °C inside the equipment's chamber using magnifications of 2000 and 7000 times.

2.4.3. Encapsulation efficiency

Quantification of the encapsulated core material (CAP) was performed by gas chromatography, and the corresponding composition was determined by GC/MS, equipped with an ion-trap mass spectrometer (TQ8040 NX Triple Quadrupole, Shimadzu, Japan), a splitless injector, an automatic sampler (AOC-20s+i), and a cross-bonded fused column (30 m×0.25 mm, 0.25 μm film thickness) for low-polarity phases (Rxi-5Sil MS, Restek, Bellefonte, USA). The equipment was operated according to a previously optimised methodology (Kessler et al., 2023). The injection port was fed with 1 μL of sample at 280 °C, with ultrapure helium flowing at 1 mL•min^{-1} under linear velocity control mode. The oven temperature was maintained at 40 °C for 1 min, then raised from 40 to 200 °C for 2 min at a rate of 7 °C•min^{-1}, followed by an increase from 200 to 250 °C for 2 min at a rate of 15 °C•min^{-1}. Subsequently, the temperature was increased to 280 °C for 1 min at 20 °C•min^{-1} for total compound separation. Mass scanning was established at *m/z* 40–500, while the ion and interface temperatures were set at 250 °C and 260 °C, respectively.

CAP identification and quantification was performed through comparison of each mass spectra molecule with those stored in the database software from the National Institute of Standards & Technology (NIST 21, 27, 107, 147).

Sample preparation consisted of taking 2 mL from the homogenized formulation, which was then combined with 1 mL of hexane and centrifugated (Micro Star 30, VWR, Pennsylvania, United States) at 3000 rpm (equivalent to 80.5 g) for 5 min. The supernatant was collected and filtered using a syringe filter (0.22 μm, 25 mm, PTFE hydrophobic, CAT 28145–495, VWR, Pennsylvania, United States), and then transferred to the injection vial (Sharkawy et al., 2017). All samples were analysed three times, and the results were quantified through the CAP calibration curve. Finally, the encapsulation efficiency (EE%) was indirectly determined by (Martins et al., 2011a; Sharkawy et al., 2017; Comunian et al., 2013):

$$EE\% = \frac{\text{total mass} - \text{nonencapsulated mass}}{\text{total mass}} \times 100 \quad (2)$$

where total mass refers to the initial CAP mass added at the start of the process, and nonencapsulated mass corresponds to the fraction of CAP that remains unencapsulated, as quantified by GC-MS.

2.4.4. Solid content

The microcapsule dispersions were submitted to an air-drying process at 105 ± 1 °C until a constant weight was achieved. This process was used to measure the solid content (SC%) gravimetrically, determined by (Hernandez-Nava et al., 2020):

$$SC\% = \frac{\text{dry mass}}{\text{liquid mass}} \times 100 \quad (3)$$

2.4.5. Fluid properties

The density and viscosity of the reagents, as well as the dispersions from each step of the microencapsulation process, were measured during batch production. These values were then used to calculate the Reynolds number for each step in the continuous mode, ensuring that it exceeds the critical Reynolds number required to achieve effective mixing. The density was measured at the respective process temperatures using a density meter with an oscillatory U-tube (DSA-4500M, Anton Paar, Graz, Austria) with an uncertainty of ± 5 × 10–5 g•mL-1 and ± 0.01 ºC. The viscosity was determined using a rheometer (MC92 RheoCompass, Anton Paar, Graz, Austria) equipped with a parallel plate (gap of 0.5 mm), also operating at the temperatures observed during each step of production.

2.5. Statistical assessment

The optimisation process for microcapsule production was conducted using two fractional factorial Design of Experiments X^{k-p}, where X is the factor, k is the number of variables for factor, and p is the factor index. In the first trial, ten experiments comprised a 3^{3-2} with 2 central points optimisation. Table 1 shows the different formulations varying the proportion of caprylic triglyceride and polysorbate 80 (CAP:P80), the stirring rate and time, and the crosslinking percentages (EDC/NHS) based on the total polymer volume used for coacervation (V_t=100 mL). The outcomes were summarised in four experiments in a second trial, with a set of 2^{3-1}, presented in Table 2.

Significant differences were assessed by ANOVA (Analysis of Variance) and Tukey tests using Statistica StatSoft (version 14, United States), at a significance level of α= 0.05 (95 % confidence). Groups were assigned different letters (e.g., a and b) to indicate statistical differences: groups sharing the same letter are not significantly different. Combined letters (e.g., ab) indicate overlap, meaning the group is statistically similar to both a and b.

3. Results

3.1. Coacervation of AG and GE

The zeta potential of the AG and GE individual polyelectrolytes and complexes was measured along with pH titration from 2 to 9, individually, as shown in Fig. 2**a**. The electrostatic forces of the anionic carboxyl groups present in the polysaccharide AG increasingly contribute to a more negative zeta potential alongside pH titration, especially in the range of 2–4. From pH 6, GE shows a zero net charge, equivalent to its isoelectric point, sustained until pH 9, meaning an equal number of positive and negative charged groups or a reduced availability of amino groups for interaction. The AG/GE curve presents a decrease from pH 2–4, mirroring the zeta potential of AG, and then stabilises throughout the titration. Previous works have found that the species contributors of each polymer in a 1:1 proportion coacervate at pH of circa 4.0 (Bastos et al., 2020; Tang et al., 2020). Thus, pH= 4 promotes the complexation of AG/GE and was therefore used to develop the cosmetic microcapsules.

Fig. 2**b** shows the FT-IR spectra for the AG/GE mixture at pH values from 2–9. At pH 2, a significant decrease in the vibrational intensity of the functional groups is observed. The wavenumber of each functional group is identified, where dashed boundaries indicate species typically found in AG (O-H, C-H, COO-symmetric and asymmetric, the fingerprint of carbohydrates (Ibekwe et al., 2017). The absorption bands of GE are identified by the shaded amide regions (Hassan et al., 2021). Fig. 2**c** shows the AG/GE mixture and the individual AG and GE spectra at pH 4. The polymer mixture predominantly reflects the AG spectrum due to its higher concentration.

3.2. Production of AG/GE microcapsules

3.2.1. Optimisation of microcapsule production in batch mode

Table 1 shows the results obtained from the first optimisation (3^{3-2} + 2 CP), comprising 10 experiments, namely D[4,3] on the first day and after 15 and 30 days, and the encapsulation efficiency (EE%). No trend was observed matching the studied variables with the resulting particle size and EE% values (ANOVA data not shown, α=0.05). Furthermore, the reliability of the data is confirmed by the absence of statistical differences in encapsulation efficiency between the two central point experiments (F5 and F10), both approximately at 91 %.

Overall, agglomeration was observed in formulations crosslinked with 1 % EDC/NHS (F1, F6, and F8), and a significant variation in particle size was observed over time for formulations developed at 13,500 rpm and 1 min (F3, F6, F9), indicating instability. Consequently, these variables were excluded from further optimisation.

For stirring rates ≤ 9500 rpm and 3–2 min, combined with a CAP:P80 ratio of 3.5 and crosslinked at 4.5–10 % (F4, F5, F10), EE% varies from 78.7 % to 99.8 % with significant differences among the samples, although without a clear trend regarding the ranged parameters. The resulting microcapsules maintained particle sizes between 49.6 to 64.4 µm over 30 days.

These results led to the second optimisation (2^{3-1}, Table 2), where CAP:P80 ratio (3.5–5.0), stirring rate and time (8000 rpm for 3 min to 9500 rpm for 2 min), and crosslinking concentration (4.5–10 %) were varied. The average particle size remained around 60 µm, with higher EE % observed for formulations performed at 9500 rpm for 2 min (ranging from 83.2 % to 88.8 %). F14 maintained a consistent particle size from the 1st to the 45th day, measuring 62.2 µm and 64.7 µm, respectively, and achieved the highest encapsulation efficiency, 88.8 %. A higher stirring rate and reduced time significantly enhanced the EE%, while no significant differences were observed in terms of SC% (α=0.05). Fig. 3

Table 1
First optimisation process for AG/GE microcapsules in terms of core material to emulsifier ratio, stirring rate and time, and crosslinking concentration.

Experiment	CAP:P80	Stirring	EDC/NHS	D[4,3] (µm)			EE%
				1st day	15th day	30th day	
F1	5.0	8000 rpm/3 min	1 %	70.1	49.5	53.9	99.8 ± 0.1a
F2	5.0	9500 rpm/2 min	10 %	59.9	33.8	34.3	94.3 ± 4.7ab
F3	5.0	13,500 rpm/1 min	4.5 %	56.1	11.3	17.3	93.6 ± 5.4ab
F4	3.5	8000 rpm/3 min	10 %	59.2	64.3	62.5	81.9 ± 5.0b
F5	3.5	9500 rpm/2 min	4.5 %	63.9	64.4	62.6	90.0 ± 1.1ab
F6	3.5	13,500 rpm/1 min	1 %	57.6	-	320.8	90.5 ± 1.2ab
F7	2.0	8000 rpm/3 min	4.5 %	125.1	86.4	50.3	96.2 ± 0.2a
F8	2.0	9500 rpm/2 min	1 %	55.2	48.2	388.8	78.7 ± 2.0b
F9	2.0	13,500 rpm/1 min	10 %	63.1	38.1	46.2	96.0 ± 0.1a
F10	3.5	9500 rpm/2 min	4.5 %	49.6	42.8	59.5	91.8 ± 0.6ab

Different letters in EE% column represent significant differences (α=0.05).
CAP:P80, proportion of caprylic triglyceride and polysorbate 80; EDC/NHS, percentage of crosslinking calculated based on polymers' solution; D[4,3], microcapsules' mean size; EE (%), encapsulation efficiency.

Table 2
Second optimisation process for AG/GE microcapsules in terms of core material to emulsifier ratio, stirring rate and time, and crosslinking concentration.

Experiment	CAP:P80	Stirring	EDC/NHS	D [4,3] (μm)		SC (%)	EE (%)
				1st day	45th day		
F11	5.0	8000 rpm/3 min	10 %	49.4	54.6	8.3 ± 0.6a	64.8 ± 5.7b
F12	3.5	8000 rpm/3 min	4.5 %	56.6	58.2	6.4 ± 0.2a	47.6 ± 3.3c
F13	5.0	9500 rpm/2 min	4.5 %	52.6	67.4	10.3 ± 0.9a	83.2 ± 0.2ab
F14	3.5	9500 rpm/2 min	10 %	62.2	64.7	8.5 ± 1.1a	88.8 ± 0.4a

Different letters in SC% and EE% columns represent significant differences (α=0.05).
CAP:P80, proportion of caprylic triglyceride and polysorbate 80; EDC/NHS, percentage of crosslinking calculated based on polymers' solution. D[4,3], microcapsules' mean size; EE (%), encapsulation efficiency.

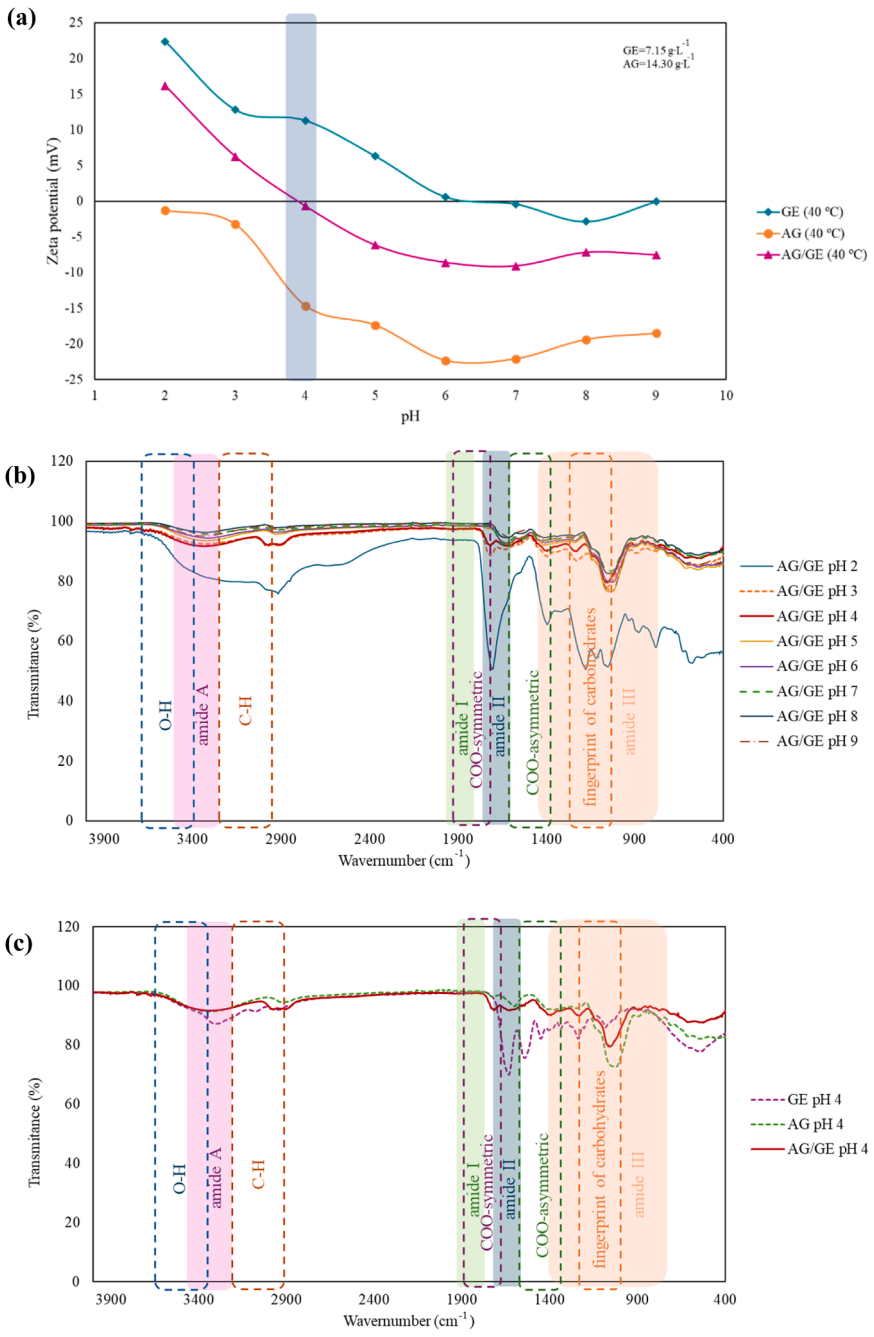

Fig. 2. Polymers' evaluation of (a) Zeta potential, (b) FT-IR of AG/GE mixture across pH range 2–9, and (c) FT-IR of the individual polymers and AG/GE mixture at pH 4.

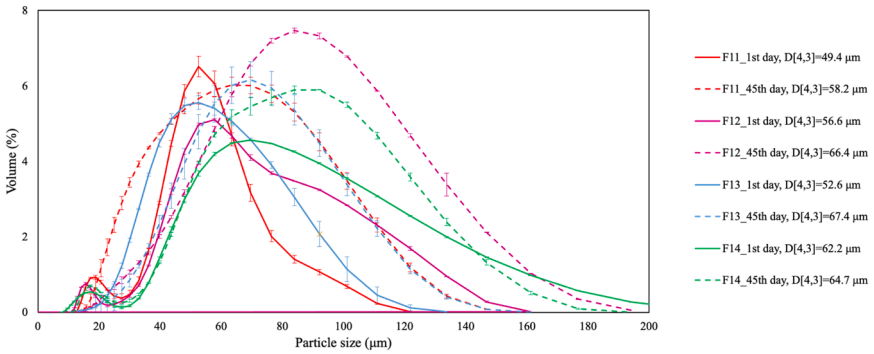

Fig. 3. Particle size distributions of microcapsule formulations (F11 to F14) produced in the second optimisation process and monitored over 45 days. Error bars represent the variation in the volume percentage (%) associated with a specific particle size range across replicate measurements.

shows the predominantly unimodal particle size distributions obtained for these experiments.

3.2.2. *Microcapsule production in continuous mode using netmix reactor*

The batch formulation F14 exhibited microcapsules with the most suitable characteristics to use as a delivery system for cosmetic ingredients due to its stability over a 45-day period, higher EE%, average SC%, and spherical shape. Therefore, it was chosen as the case study to transfer for continuous mode production.

The fluid-dynamic properties, density and viscosity, of the reagents and of the resulting solutions (emulsion or dispersions), were measured at each step of the microcapsule production during batch mode operation and are reported in Supplementary Material 2. The density was approximately 1 g•cm^{-3} and all solutions exhibited Newtonian behaviour. The viscosity values were measured at 2.04 mPa•s in step 1, 1.39 mPa•s in step 2, 2.34 mPa•s in step 4 and 1.73 mPa•s in step 5. Higher viscosity values of 3.28 mPa•s and 45.8 mPa•s was observed in steps 6 and 7, which were not transposed to continuous operation. The operational flow rate was set at circa 307 mL·min^{-1} in step 1 and 326 mL·min^{-1} in step 2, resulting in Reynolds numbers of 355 and 559, respectively.

Table 3 shows the conditions and results for four experiments performed in continuous mode (all experiments were duplicated). In all experiments, steps 1 and 2 were performed using NETmix for reactant mixing and recirculation, while step 3 was always done using only a stirrer. Steps 4 and 5 were carried out under different conditions to study the effect of using NETmix compared to stirrer. In experiment E2, both NETmix and a stirrer were used in step 4, yielding similar results to E1 in terms of particle size (52.7 μm and 56.8 μm), SC% (6.3 % and 5.7 %), and EE% (96.3 % and 97.7 %). In experiment E3, the combination NETmix and a stirrer was also used in step 5 (as shown in Supplementary Material 3). This resulted in a significant decrease in particle size (42.5 μm), with similar values for SC% (5.7 %) and EE% (98.2 %). Finally, in experiment E4, the production of microcapsules was attempted using only NETmix in step 4. This led to a significantly larger particle size (102.0 μm), and lower values for SC% (4.8 %) and EE% (85.2 %). This setup evidenced the limitations of using NETmix without the assistance of a magnetic stirrer.

Table 3
Continuous production of AG/GE microcapsules in the NETmix micro-reactor based on batch-optimised F14 parameters.

Experiment	Step 4	Step 5	D [4,3] (μm)	SC (%)	EE (%)
E1	Stirrer	Stirrer	52.7 ± 0.7c	6.3 ± 0.1a	96.3 ± 1.7a
E2	Stirrer + NETmix	Stirrer	56.8 ± 1.0b	5.7 ± 0.6a	97.7 ± 0.6a
E3	Stirrer + NETmix	Stirrer + NETmix	42.5 ± 0.8d	5.7 ± 0.1a	98.2 ± 1.5a
E4	NETmix	Stirrer + NETmix	102.0 ± 1.0a	4.9 ± 0.3a	85.2 ± 2.2b

Different letters in D[4,3], SC%, and EE% columns represent significant differences (α=0.05).
D[4,3], microcapsules' mean size.

3.3. *Microcapsules morphology characterisation*

3.3.1. *Morphology of the microcapsules produced in batch mode*

The formulations resulting from the optimisation procedures underwent a series of microscopy assessments, focusing particularly on those generated in the second Design of Experiments. Fig. 4 shows optical microscopy images of the produced microcapsules on the first day and after 45 days, where a similar average particle size of 60 μm is observed. The morphology of the microcapsules was confirmed through confocal microscopy. The polymer phase is shown in blue in Fig. 5**i,** and the oil phase in red in **Figure 5ii**. The overlapping layers of the two materials are shown in **Figure 5iii,** where the pink spots indicate the presence of microencapsulated oil scattered randomly throughout the structure. A consistent pattern is observed for all four formulations, with the oil phase dispersed within the porous material. The formation of three-dimensional structures containing dispersed oil droplets within the porous material is confirmed in Fig. 6**i-iii**. These panels display images captured from successive layers or focal planes within the same analysis area, providing a clear depiction of the system's multilayered architecture. The observation of oil droplets across the focal planes confirms the structural integrity and composition of the microcapsules, as well as its three-dimensional structure and multinucleated nature. A video animation of these images is presented in Supplementary Material 4.

Cryo-SEM images of the produced microcapsules are shown in Fig. 7. This imaging technique preserves the original structure of the microcapsules (Martins et al., 2009), focusing on either the inner core or the outer layer. The images display a honeycomb-like structure surrounding the oil phase, with a uniform polymeric coating enveloping the entire microparticle. This configuration not only protects the active ingredient from environmental stresses but also potentially affects its release rate, thereby influencing the delivery system's performance.

In summary, image analyses revealed a spherical delivery system with a multinucleated morphology, featuring CAP within a porous structure covered by a dense polymeric shell with an average particle size of circa 60 μm, unchanged during the 45-day storage period.

The porous polymer structure shows favourable attributes as a candidate for encapsulating different target compounds relevant for cosmetic applications, with sizes comparable to those of previous AG/GE coacervates (Shaddel et al., 2018).

3.3.2. *Morphology of the microcapsules produced in continuous mode*

All products were evaluated by optical microscopy, leading to new

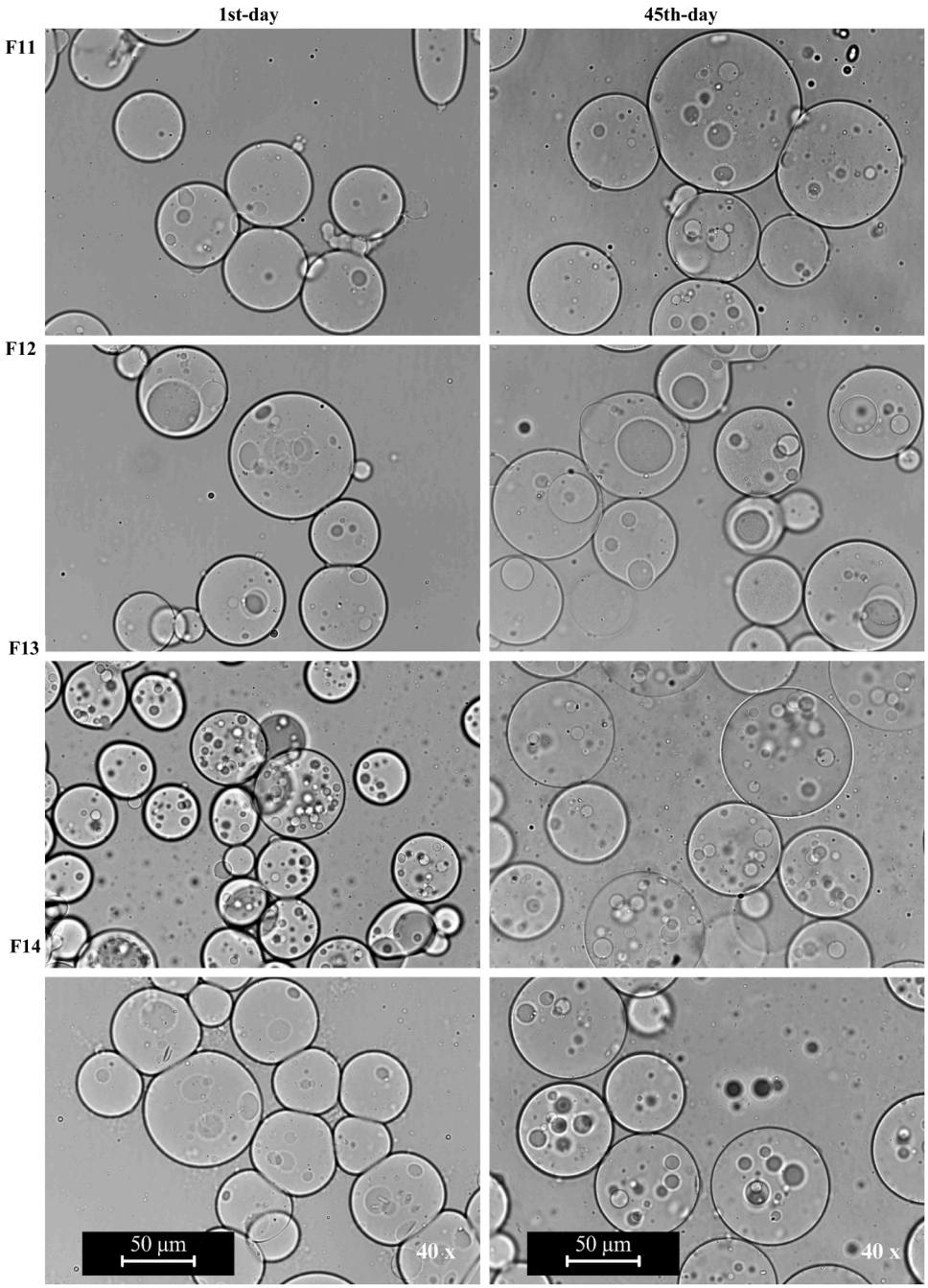

Fig. 4. Optical microscopy of microcapsules produced in the second optimisation process monitored over a period of 45 days.

findings (Fig. 8). Experiments E1 and E2 feature spherical and regular shapes within particle sizes of 52.7 µm and 56.8 µm, respectively. Both experiments used a magnetic stirrer at 400 rpm for 60 min to crosslink the microcapsules dropwise with EDC/NHS.

In the images from trials E3 and E4, microcapsules with spherical shapes are observed, although they exhibit some irregular structures. These irregularities may result from the rupture of the microcapsules (experiment E3), or due to potential limitations in polymer coacervation (experiment E4). The images also help to explain the particle sizes obtained: in E3, the lower average particle size is due to the presence of broken particles, whereas in E4, the particles seem to agglomerate, leading to a higher average particle size. These results show the importance and significant influence of steps 4 and 5, cooling and hardening, respectively. The limitation on transitioning the entire process to continuous mode is likely due to substantial mechanical impact on the microcapsules formed in step 3, in which the microcapsules are still coacervating and presenting free and reactive amino groups (Adamiak & Sionkowska, 2020) (see section 4.3).

Using the continuous mode, the production of cosmetic microcapsules achieved approximately a 9 % increase in encapsulation efficiency and an 8 % reduction in operational time compared to the batch mode.

3.4. Chemical characterisation of microcapsules core material (CAP) and encapsulation efficiency

The analysis of the core material (CAP) chemical composition is shown in Table 4 and indicates the presence of four fatty acids obtained through coconut oil esterification. Among these, caprylic acid ($C_{8:0}$) predominates with a relative concentration of 43.4 %, leading to the product's naming. Capric ($C_{10:0}$) and caproic acids ($C_{6:0}$) are also present

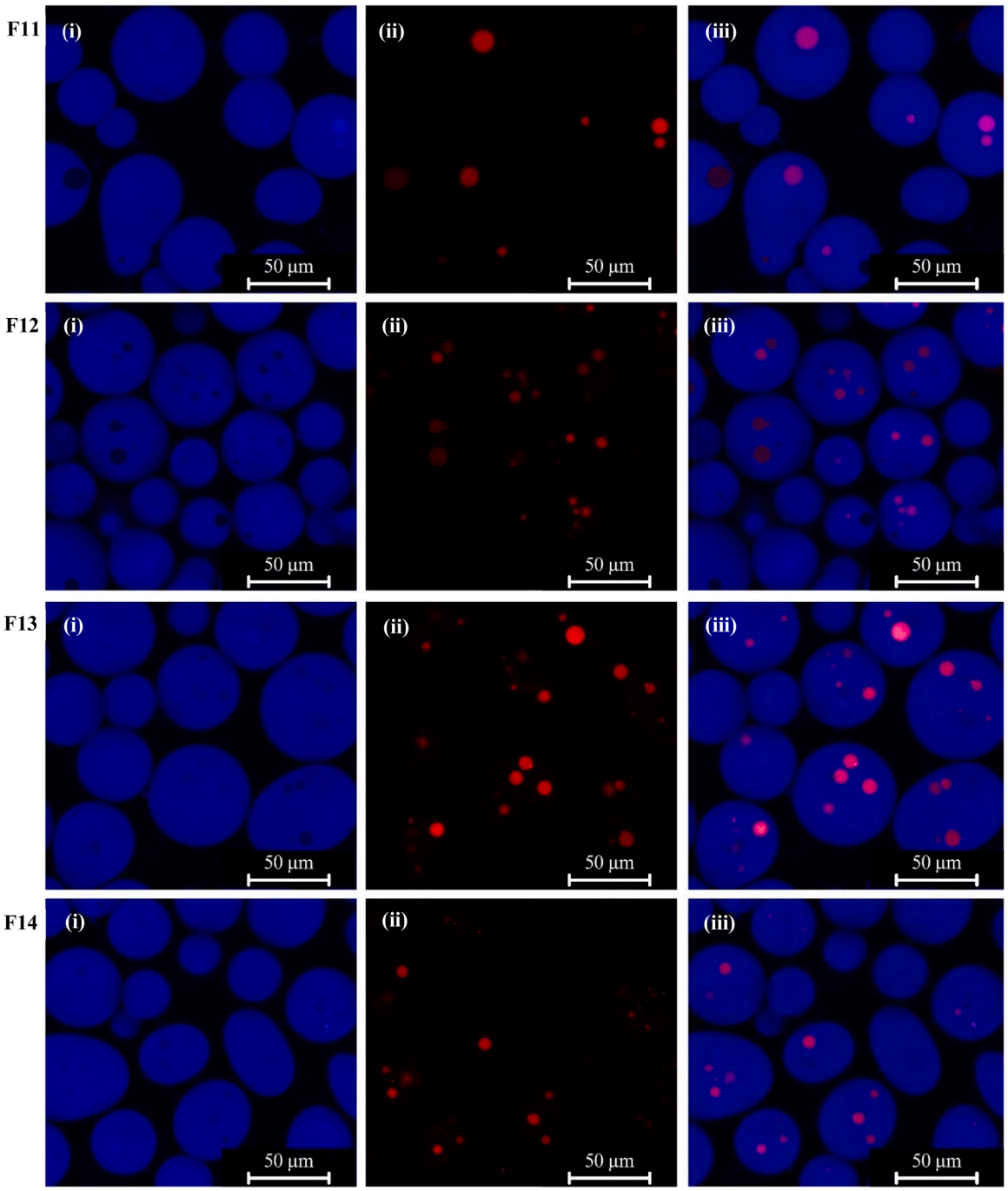

Fig. 5. Confocal microscopy of microcapsules produced in the second optimisation process, where (i) represents the hydrophilic polymeric phase or shell material, (ii) identifies the hydrophobic phase CAP or core material, and (iii) indicates overlap between both shell and core materials.

at 29.2 % and 22.6 %, respectively, while lauric acid ($C_{12:0}$) is responsible for only 4.7 % of the total composition.

The chemical composition of the encapsulated material in formulations F11 to F14 was also analysed, as shown in Table 4. For easier comparison, the encapsulation efficiency of each compound is expressed relative to the overall EE% for each formulation (Table 2). The identified compounds showed consistent behaviour across experiments F11 to F14, with no significant differences in the relative composition compared with CAP alone. However, F14 featured the highest similarity to CAP and achieved the highest total EE% (Table 2).

4. Discussion

4.1. Production of microcapsules in batch mode

4.1.1. Emulsifier effect

The concentration of emulsifier in the system is a key factor influencing the formation and stability of droplets in oil-in-water mixtures. During emulsification, droplet size and stability are determined by the delicate balance between opposing forces: turbulent forces, which break droplets into smaller sizes, and interfacial tension forces, which resist this breakup and work to maintain droplet integrity. An optimal emulsifier concentration ensures that these forces are balanced, promoting stable droplet formation and preventing coalescence or phase separation

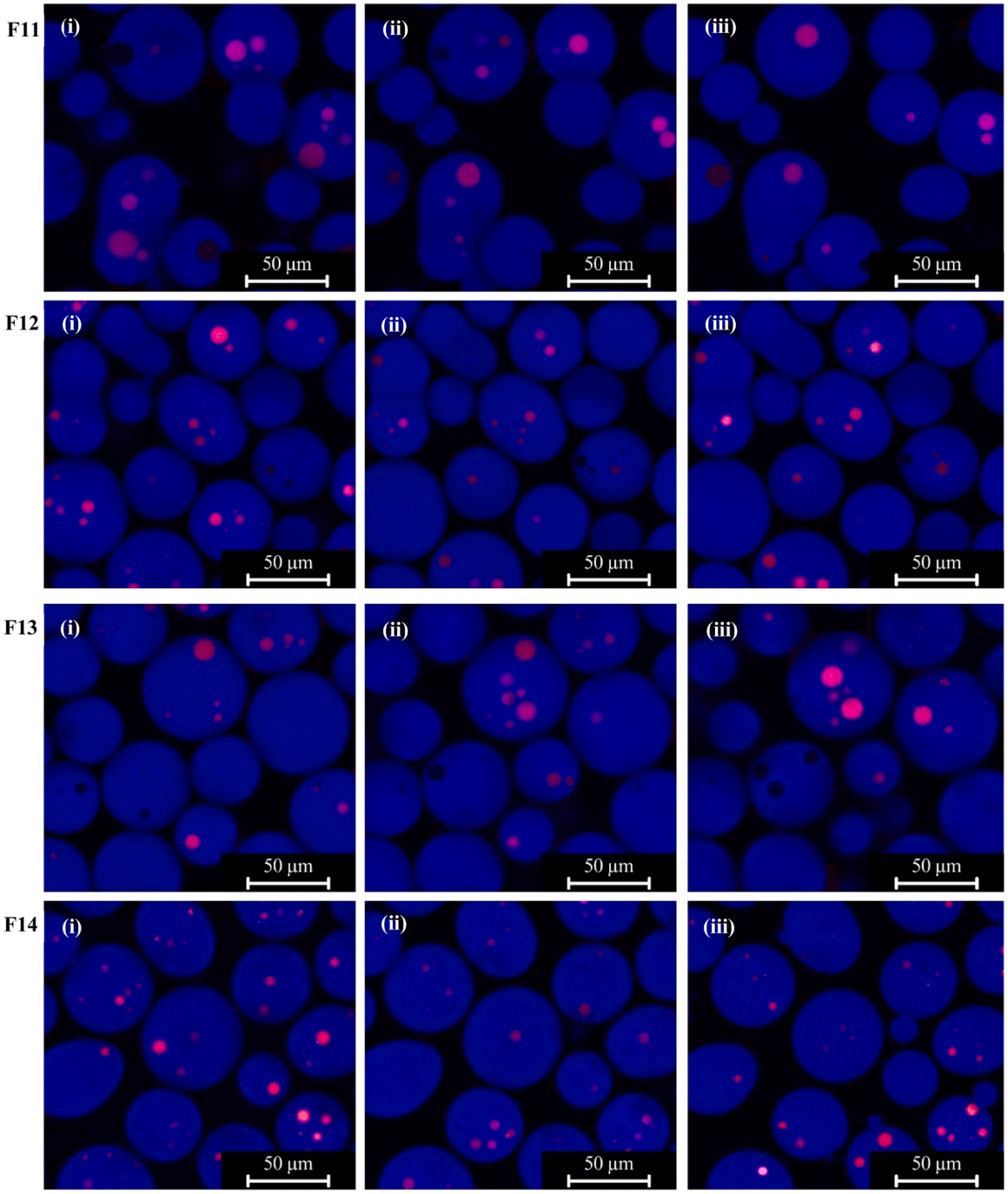

Fig. 6. Confocal microscopy images of microcapsules produced during the second optimisation process. Panels (i) to (iii) show sequential focal planes of the same analysis area.

(Butstraen & Salaün, 2014). The literature claims that AG's emulsifier properties lead to stabilisation by increased viscosity due to its high molecular mass (da Silva et al., 2015). The arabinogalactan-protein fraction conditions AG's ability to stabilise oil-in-water (o/w) emulsions, the main polysaccharide complex in AG composition, also influencing droplet individualisation (Desplanques et al., 2012). The literature indicates emulsification occurs either in the absence or deliberate exclusion of an amphiphilic agent (da Silva et al., 2015; Dong et al., 2011; Lv et al., 2013).

In this study, preliminary trials without the use of an emulsifier (data not shown) did not result in the formation of microcapsules. Emulsifiers have proven to be effective in stabilising emulsion prior to coacervation. Although stabilisers with high hydrophilic-lipophilic balance (HLB=9.6–17.6) are typically used in water-in-oil (w/o) emulsions (Martins et al., 2011a; Sharkawy et al., 2017), microencapsulation processes (o/w) have shown a significant dependency on the encapsulated material. Enhanced efficiencies in encapsulating hydrophobic compounds were obtained in AG/GE systems by using emulsifiers with HBL ranging from 1.8 to 6.7 (Rabisková & Valásková, 2008). Therefore, P80 (HBL_{P80}=4.3) was chosen as an emulsifier, and its use was limited to the minimum quantity necessary to produce self-sustaining microparticles based on the optimisations shown in Table 1 and Table 2. The stabilisation was efficiently achieved using a proportion CAP:P80 of 3.5:1, which is more than four times lower compared to previous AG/GE

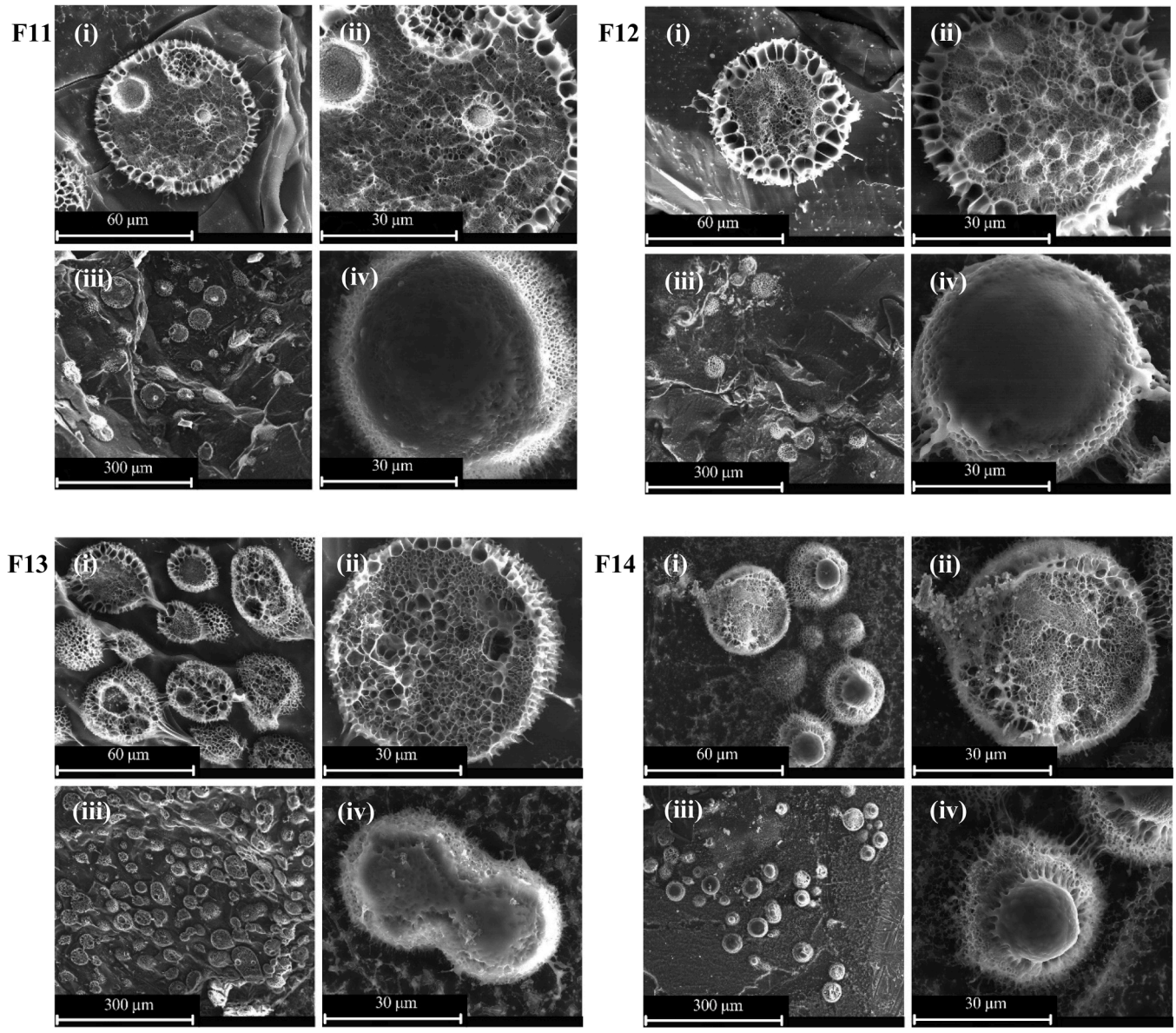

Fig. 7. Cryo-Scanning Electron Microscopy images of microcapsules produced in the second optimisation process (formulations F11 to F14) at magnifications of 2000x (i and iii) and 7000x (ii and iv), where (i and ii) show the inner core, and (iii and iv) show the outer layer.

microparticles stabilised by a blend of surfactants containing P80 (0.85:1) (Yue et al., 2022).

Alternative emulsifiers to P80, such as PGPR (polyglycerol polyricinoleate), have been used in the development of AG/GE coacervates (Comunian et al., 2013; Shaddel et al., 2018). PGPR, which has a similar HLB to P80 (HBL_{PGPR}=4.5), also resulted in multinucleated microparticles, with particle sizes from 52 to 84 µm (Comunian et al., 2013) and 35–80 µm (Shaddel et al., 2018). Non-ionic surfactants with low HLB values (PGPR and sorbitan trioleate), identified as promoters of higher encapsulation efficiency for hydrophobic core materials in AG/GE coacervation (Rabisková & Valásková, 2008), have also been used in the microencapsulation of vanillin and limonene (Sharkawy et al., 2017).

4.1.2. Stirring rate effect

A higher emulsification stirring rate is commonly anticipated to lead to a reduction in particle size. For example, a study on camphor AG/GE microcapsules showed that the particle size decreased from 295 to 86 µm when the stirring rate was increased from 500 to 2000 rpm (Chang et al., 2006). Similar findings are indicated for flavour coacervates, in which the particle size reduced from 82.7 to 67.1 µm by increasing the stirring rate from 3000 to 9000 rpm (Yeo et al., 2005).

In this work, a relatively narrow range of stirring rates, between 8000 and 9500 rpm, led to stable microcapsules with high encapsulation efficiency. After 45 days of storage, particle sizes ranged between 54.6 and 67.4 µm, with the higher values observed when using 9500 rpm (see Table 2). A higher stirring rate of 13,500 rpm was tested, leading in most cases to non-stable microcapsules over a 30-day storage period.

Stirring time, pH-dependency, and polymers' concentration are also highly associated with the particle size of coacervates (da Silva et al., 2015; Marfil et al., 2018). This suggests that the size of the coacervates is likely influenced by a combination of factors rather than solely by the stirring rate.

4.1.3. Crosslinking concentration effect

Crosslinkers can improve GE coacervate's thermal and mechanical stability (Kuijpers et al., 2000). Aldehydes, such as formaldehyde and glutaraldehyde, are commonly used in the crosslinking stages of cosmetic microcapsules (Chang et al., 2006; Prata et al., 2008; Yue et al.,

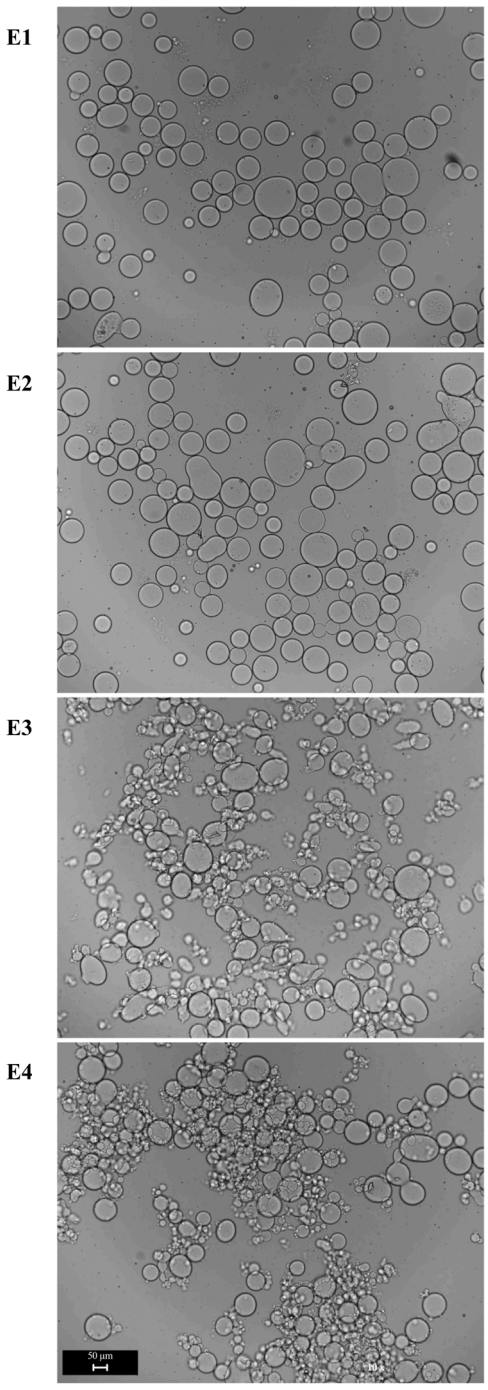

Fig. 8. Optical microscopy of microcapsules produced in continuous mode using the mesostructured micro-reactor NETmix.

2022) but have been recognised as toxic and were not used in this work. A mixture of EDC/NHS was chosen since this combination of compounds is a zero-length crosslinker, and it operates by activating carboxylic acid residues to react with free amino residues only through direct amide covalent bonds (Kuijpers et al., 2000). Furthermore, EDC/NHS does not leave any linker or spacer, successfully mimics enzymes stabilising the collagen structure, and is biocompatible and non-cytotoxic (Adamiak & Sionkowska, 2020).

In this work, the produced microcapsules showed a dependency upon the concentration of crosslinker, mainly influencing the stability of the microparticles over time (Table 1). Formulations crosslinked using only 1 % of EDC/NHS favoured agglomeration, likely associated with

Table 4
Chemical profile of core material (CAP) and encapsulation efficiency of identified compounds for formulation F11-F14 from the second optimisation process.

Compound	Relative concentration (%) CAP	EE%			
		F11	F12	F13	F14
Caproic acid ($C_{6:0}$)	22.6 ± 1.4ab	20.8 ± 1.7b	20.4 ± 1.4b	21.9 ± 0.3b	23.8 ± 0.2a
Caprylic acid ($C_{8:0}$)	43.4 ± 2.2ab	40.5 ± 3.3b	40.1 ± 2.8b	41.8 ± 0.6b	41.2 ± 1.7a
Capric acid ($C_{10:0}$)	29.2 ± 1.9a	30.8 ± 2.5a	30.9 ± 2.2a	30.2 ± 0.4a	30.1 ± 0.2a
Lauric acid ($C_{12:0}$)	4.7 ± 1.7ab	7.9 ± 0.7a	8.6 ± 0.6a	6.1 ± 0.1b	5.0 ± 0.0b

Different letters in each compound line represent significant differences (α=0.05).
CAP, caprylic triglyceride.

the quantity of free amino acid groups remaining after coacervation. Originally, gelatine A has 31.5 ± 2.5 free amino acid groups per 1000 amino acids, which can be consumed by chemical crosslinking (Kuijpers et al., 2000). Concentrations of 4.5 % and 10 % led to stable microcapsules after 45-day storage with no significative particle size differences (Table 2).

4.2. Microcapsules continuous production using NETmix reactor

The continuous production of microcapsules has been successfully performed using NETmix. This is the first time that MCC has been introduced with the NETmix mesostructured reactor.

Similar to a previous study on melamine-formaldehyde microcapsules containing Miglyol (analogous to CAP) produced by polycondensation in NETmix (Moreira et al., 2020), in this work microcapsules resembling the morphological characteristics and encapsulation efficiency of the optimised batch formulation were obtained. The melamine-formaldehyde microcapsules were sized circa 40 µm, with up to 70 % encapsulation efficiency, and most significantly, a reduction of processing time from 120 to 30 min using Re of approximately 200. Although both systems operated above the critical Reynolds number, the continuous mode MCC process (Re > 300) did not significantly reduce processing time due to limitations imposed by the cooling and hardening steps, which remained batch dependent. However, transitioning the emulsification and polymer addition steps to a continuous mode introduced significant improvements in encapsulation efficiency. This enhancement can be attributed to the optimised flow dynamics in the continuous process, which facilitated more consistent and controlled droplet formation. The improved droplet uniformity ensured better interaction between the dispersed phase and the polymers, promoting a more efficient encapsulation process. Additionally, the continuous flow environment likely reduces variability and allows for tighter control over the physical and chemical interactions critical for encapsulation, therefore leading to superior performance.

Previous works have shown challenges related to the hardening step for the production of AG/GE microcapsules by MCC in batch mode, with no microcapsule formation observed when the crosslinking time is less than 60 min (Junyaprasert et al., 2001). New trials studying the effect of the Reynolds numbers during recirculation or considering the substitution of the peristaltic pump to avoid friction and particle disruption are worthwhile avenues for experimentation.

5. Conclusions

The tailored microcapsules for integration into cosmetic formulations were successfully developed. Through the coacervation of Arabic gum and gelatine A, the encapsulation of caprylic acid to carry a variety of hydrophobic bioactives was proposed, aiming to protect their

functional properties with improved efficacy on the skin. Dual optimisation endeavours led to the creation of spherical microcapsules with a multinucleated morphology, as evidenced by imaging analyses. Remarkably, these characteristics remained stable over 45 days, suggesting enhanced durability and functionality for extended use in cosmetic formulations. High encapsulation efficiency and particles of suitable size for cosmetic use were achieved by combining a 3.5:1 emulsifier-to-carrier ratio, 9500 rpm stirring rate, and 10 % crosslinking concentration.

Furthermore, the achievements of this study were extended beyond formulation optimisation; this study successfully scaled the process up by harnessing the capabilities of a mesostructured microreactor, the NETmix. Due to the limitations of the laboratory scale NETmix setup used, this study required the recirculation of the solution and a magnetic stirrer to maintain solution homogeneity. However, the process can be transitioned into continuous mode by increasing the reactor size (number of rows) or coupling multiple reactors in series. This advancement in production technology ensures consistency in product quality and lays the groundwork for future activities in large-scale manufacturing.

Microencapsulation in cosmetic innovation holds promise for improving formulation standards and expanding possibilities in beauty enhancement. The advancements demonstrated in this work for the continuous production of microcapsules highlight the commercial viability of MCC as a delivery system in cosmetic applications. Future work includes the encapsulation of various hydrophobic bioactives featuring *Moringa oleifera* leaf extracts obtained by carbon dioxide supercritical extraction, release and permeation assessments, incorporation into commercial hydrating creams, and human volunteer skin tests to validate the real-world application.

CRediT authorship contribution statement

Dias Madalena Maria: Writing – review & editing, Validation, Supervision, Project administration, Funding acquisition, Conceptualization. **Kessler Júlia Cristiê:** Writing – original draft, Methodology, Investigation, Data curation, Conceptualization. **Martins Isabel Maria:** Writing – review & editing, Methodology, Formal analysis, Data curation. **Rodrigues Alírio Egídio:** Writing – review & editing, Supervision, Methodology, Conceptualization. **Barreiro Maria Filomena:** Writing – review & editing, Validation, Supervision, Methodology, Funding acquisition. **Manrique Yaidelin Alves:** Validation, Methodology, Investigation, Data curation. **Lopes José Carlos B.:** Writing – review & editing, Validation, Methodology.

Declaration of Competing Interest

The authors declare that they have no known competing financial interests or personal relationships that could have appeared to influence the work reported in this paper.

Acknowledgements

This work was supported by national funds through FCT/MCTES (PIDDAC): LSRE-LCM, UIDB/50020/2020 (DOI: 10.54499/UIDB/50020/2020) and UIDP/50020/2020 (DOI: 10.54499/UIDP/50020/2020); ALiCE, LA/P/0045/2020 (DOI: 10.54499/LA/P/0045/2020); CIMO, UIDB/00690/2020 (DOI: 10.54499/UIDB/00690/2020) and UIDP/00690/2020 (DOI: 10.54499/UIDP/00690/2020); and LA SusTEC, LA/P/0007/2021 (DOI:10.54499/LA/P/0007/2020). Júlia Cristiê Kessler acknowledges her PhD scholarship (ref. 2020.06656.BD, DOI: 10.54499/2020.06656.BD) from FCT.

Appendix A. Supporting information

Supplementary data associated with this article can be found in the online version at doi:10.1016/j.cherd.2025.01.035.

References

Adamiak, K., Sionkowska, A., 2020. Current methods of collagen cross-linking: Review. Int. J. Biol. Macromol. 161, 550–560. https://doi.org/10.1016/j.ijbiomac.2020.06.075.

Ang, L.F., Darwis, Y., Koh, et al., 2019. Wound Healing property of curcuminoids as a microcapsule-incorporated cream. Pharmaceutics 11, 205 https://www.mdpi.com/1999-4923/11/5/205.

Bastos, L.P.H., Vicente, J., et al., 2020. Encapsulation of black pepper (*Piper nigrum* L.) essential oil with gelatin and sodium alginate by complex coacervation. Food Hydrocoll. 102, 105605. https://doi.org/10.1016/j.foodhyd.2019.105605.

Butstraen, C., Salaün, F., 2014. Preparation of microcapsules by complex coacervation of gum Arabic and chitosan. Carbohydr. Polym. 99, 608–616. https://doi.org/10.1016/j.carbpol.2013.09.006.

Carpentier, J., Conforto, E., et al., 2022. Microencapsulation and controlled release of α-tocopherol by complex coacervation between pea protein and tragacanth gum: A comparative study with arabic and tara gums. IFSET 77, 102951. https://doi.org/10.1016/j.ifset.2022.102951.

Carvalho, I.T., Estevinho, B.N., Santos, L., 2016. Application of microencapsulated essential oils in cosmetic and personal healthcare products – a review. Int. J. Cosmet. Sci. 38, 109–119. https://doi.org/10.1111/ics.12232.

Chang, Leung, C.-P., Lin, T.-K., et al., 2006. Release properties on gelatin-gum arabic microcapsules containing camphor oil with added polystyrene. Colloids Surf. B Biointerfaces 50, 136–140. https://doi.org/10.1016/j.colsurfb.2006.04.008.

Comunian, T.A., Thomazini, M., et al., 2013. Microencapsulation of ascorbic acid by complex coacervation: Protection and controlled release. Food Res. Int. 52, 373–379. https://doi.org/10.1016/j.foodres.2013.03.028.

da Silva, B.C., de Oliveira, M., et al., 2015. Polyelectrolyte complexes from gum arabic and gelatin: Optimal complexation pH as a key parameter to obtain reproducible microcapsules. Food Hydrocoll. 46, 201–207. https://doi.org/10.1016/j.foodhyd.2014.12.022.

Desplanques, S., Renou, F., et al., 2012. Impact of chemical composition of xanthan and acacia gums on the emulsification and stability of oil-in-water emulsions. Food Hydrocoll. 27, 401–410. https://doi.org/10.1016/j.foodhyd.2011.10.015.

Dong, Z., Ma, Y., et al., 2011. Morphology and release profile of microcapsules encapsulating peppermint oil by complex coacervation. J. Food Eng. 104, 455–460. https://doi.org/10.1016/j.jfoodeng.2011.01.011.

Fernandes, I.S., Brito, M.S.C.A., et al., 2023. Experimental and numerical characterisation of two-phase flow in NETmix reactors. Chem. Eng. Process. 194, 109580. https://doi.org/10.1016/j.cep.2023.109580.

Ferreira, S., Nicoletti, V.R., 2021. Use of a tubular heat exchanger to achieve complex coacervation in a semi-continuous process: Effects of capsules curing temperature and shear rate. J. Food Eng. 310, 110698. https://doi.org/10.1016/j.jfoodeng.2021.110698.

Hassan, N., Ahmad, T., et al., 2021. Identification of bovine, porcine and fish gelatin signatures using chemometrics fuzzy graph method. Sci. Rep. 11, 9793. https://doi.org/10.1038/s41598-021-89358-2.

Hernandez-Nava, R., López-Malo, A., et al., 2020. Encapsulation of oregano essential oil (Origanum vulgare) by complex coacervation between gelatin and chia mucilage and its properties after spray drying. Food Hydrocoll. 109, 106077. https://doi.org/10.1016/j.foodhyd.2020.106077.

Ibekwe, C.A., Oyatogun, G.M., et al., 2017. Synthesis and characterization of chitosan/gum arabic nanoparticles for bone regeneration. Am. J. Mater. Sci. Eng. 5, 28–36. https://doi.org/10.12691/ajmse-5-1-4.

Junyaprasert, V.B., Mitrevej, A., et al., 2001. Effect of process variables on the microencapsulation of vitamin a palmitate by gelatin-acacia coacervation. Drug Dev. Ind. Pharm. 27, 561–566. https://doi.org/10.1081/DDC-100105181.

Kessler, J.C., Manrique, Y.A., et al., 2023. *Moringa oleifera* L. screening: SFE-CO_2 optimisation and chemical composition of seed, leaf, and root extracts as potential cosmetic ingredients. Separations 10, 210 https://www.mdpi.com/2297-8739/10/3/210.

Kessler, J.C., Martins, I.M., et al., 2024. Advancements in conventional and supercritical CO_2 extraction of *Moringa oleifera* bioactives for cosmetic applications: A review. J. Supercrit. Fluids, 106388. https://doi.org/10.1016/j.supflu.2024.106388.

Kuijpers, A.J., Engbers, G.H.M., et al., 2000. Cross-linking and characterisation of gelatin matrices for biomedical applications. J. Biomater. Sci. Polym. Ed. 11, 225–243. https://doi.org/10.1163/156856200743670.

Laranjeira, P.E., Martins, A.A., et al., 2009. NETmix®, a new type of static mixer: Modeling, simulation, macromixing, and micromixing characterization. AIChE J. 55, 2226–2243. https://doi.org/10.1002/aic.11815.

Laranjeira, P.E., Martins, A.A., et al., 2011. NETmix®, a new type of static mixer: Experimental characterization and model validation. AIChE J. 57, 1020–1032. https://doi.org/10.1002/aic.12316.

Li, L., Au, W., et al., 2013. Improvement in antibacterial activity of moxa oil containing gelatin-arabic gum microcapsules. Text. Res. J. 83, 1236–1241. https://doi.org/10.1177/0040517512467059.

Lopes, J.C.B., Laranjeira, P.E., et al., 2005. Network mixer and related mixing process. Faculdade de Engenharia da Universidade do Porto.

Lv, Y., Zhang, X., et al., 2013. The study of pH-dependent complexation between gelatin and gum arabic by morphology evolution and conformational transition. Food Hydrocoll. 30, 323–332. https://doi.org/10.1016/j.foodhyd.2012.06.007.

Marfil, P., Paulo, B., et al., 2018. Production and characterization of palm oil microcapsules obtained by complex coacervation in gelatin/gum Arabic. J. Food Process Eng. 41, e12673. https://doi.org/10.1111/jfpe.12673.
Marques, M.P., Sanchez-Salvador, J.L., et al., 2024. Development of o/w pickering emulsions stabilized with leek leaf trimmings using batch and continuous modes. Food Bioproc. Tech. https://doi.org/10.1007/s11947-023-03296-7.
Martins, I.M., Barreiro, M.F., et al., 2014. Microencapsulation of essential oils with biodegradable polymeric carriers for cosmetic applications. Chem. Eng. J. 245, 191–200. https://doi.org/10.1016/j.cej.2014.02.024.
Martins, I.M., Rodrigues, S.N., et al., 2009. Microencapsulation of thyme oil by coacervation. J. Microencapsul. 26, 667–675. https://doi.org/10.3109/02652040802646599.
Martins, I.M., Rodrigues, S.N., et al., 2011a. Polylactide-Based thyme oil microcapsules production: evaluation of surfactants. Ind. Eng. Chem. Res. 50, 898–904. https://doi.org/10.1021/ie101815f.
Martins, I.M., Rodrigues, S.N., et al., 2011b. Release of thyme oil from polylactide microcapsules. Ind. Eng. Chem. Res. 50, 13752–13761. https://doi.org/10.1021/ie200791r.
Matos, J., Santos, R.J., et al., 2024. Chaos and mixing in NETmix. AIChE J. 70, e18461. https://doi.org/10.1002/aic.18461.
Moreira, A.C.G., Manrique, Y.A., et al., 2020. Continuous production of melamine-formaldehyde microcapsules using a mesostructured reactor. Ind. Eng. Chem. Res. 59, 18510–18519. https://doi.org/10.1021/acs.iecr.0c02656.
Moreira, A.C.G., Manrique, Y.A., et al., 2022. Continuous production of cellulose acetate microspheres for textile impregnation using a mesostructured reactor. Cellulose 29, 3595–3612. https://doi.org/10.1007/s10570-022-04513-w.
Muhoza, B., Xia, S., et al., 2020. Microencapsulation of essential oils by complex coacervation method: preparation, thermal stability, release properties and applications. Crit. Rev. Food Sci. Nutr. 1363–1382. https://doi.org/10.1080/10408398.2020.1843132.
Prata, A.S., Grosso, C.R.F., 2015. Influence of the oil phase on the microencapsulation by complex coacervation. JAOCS 92, 1063–1072. https://doi.org/10.1007/s11746-015-2670-z.
Prata, A.S., Zanin, M.H., et al., 2008. Release properties of chemical and enzymatic crosslinked gelatin-gum Arabic microparticles containing a fluorescent probe plus vetiver essential oil. Colloids Surf. B Biointerfaces 67, 171–178. https://doi.org/10.1016/j.colsurfb.2008.08.014.
Rabisková, M., Valásková, J., 2008. The influence of HLB on the encapsulation of oils by complex coacervation. J. Microencapsul. 15, 747–751. https://doi.org/10.3109/02652049809008257.
Ribeiro, A., Manrique, Y.A., et al., 2021. Continuous production of hydroxyapatite Pickering emulsions using a mesostructured reactor. Colloids Surf. A: Physicochem. Eng. Asp. 616, 126365. https://doi.org/10.1016/j.colsurfa.2021.126365.
Schneider, C.A., Rasband, W.S., Eliceiri, K.W., 2012. NIH Image to ImageJ: 25 years of image analysis. Nat. Methods 9, 671–675. https://doi.org/10.1038/nmeth.2089.
Shaddel, R., Hesari, J., et al., 2018. Use of gelatin and gum Arabic for encapsulation of black raspberry anthocyanins by complex coacervation. Int. J. Biol. Macromol. 107, 1800–1810. https://doi.org/10.1016/j.ijbiomac.2017.10.044.
Sharkawy, A., Fernandes, I.P., et al., 2017. Aroma-loaded microcapsules with antibacterial activity for eco-friendly textile application: Synthesis, characterization, release, and green grafting. Ind. Eng. Chem. Res. 56, 5516–5526. https://doi.org/10.1021/acs.iecr.7b00741.
Tang, Y., Scher, H.B., Jeoh, T., 2020. Industrially scalable complex coacervation process to microencapsulate food ingredients. IFSET 59, 102257. https://doi.org/10.1016/j.ifset.2019.102257.
Taofiq, O., González-Paramás, A.M., et al., 2016. Mushrooms extracts and compounds in cosmetics, cosmeceuticals and nutricosmetics-A review. Ind. Crops Prod. 90, 38–48. https://doi.org/10.1016/j.indcrop.2016.06.012.
Timilsena, Y.P., Akanbi, T.O., et al., 2019. Complex coacervation: Principles, mechanisms and applications in microencapsulation. Int. J. Biol. Macromol. 121, 1276–1286. https://doi.org/10.1016/j.ijbiomac.2018.10.144.
Xiao, Z., Liu, W., et al., 2014. A review of the preparation and application of flavour and essential oils microcapsules based on complex coacervation technology. J. Sci. Food Agric. 94, 1482–1494. https://doi.org/10.1002/jsfa.6491.
Yang, W., Gong, Y., et al., 2024. Design of gum Arabic/gelatin composite microcapsules and their cosmetic applications in encapsulating tea tree essential oil. RSC Adv. 14, 4880–4889. https://doi.org/10.1039/d3ra08526k.
Yeo, Y., Bellas, E., et al., 2005. Complex coacervates for thermally sensitive controlled release of flavor compounds. J. Agric. Food Chem. 53, 7518–7525. https://doi.org/10.1021/jf0507947.
Yue, Y., Xin, G., et al., 2022. Chemical composition, antimicrobial activities and microencapsulation by complex coacervation of tea tree essential oils. J. Process. Preserv. 46, e16585. https://doi.org/10.1111/jfpp.16585.
Zhang, Z.-Q., Pan, C.-H., Chung, D., 2011. Tannic acid cross-linked gelatin–gum arabic coacervate microspheres for sustained release of allyl isothiocyanate: Characterization and in vitro release study. Food Res. Int. 44, 1000–1007. https://doi.org/10.1016/j.foodres.2011.02.044.
Zuanon, L.A.C., Malacrida, C.R., Telis, V.R.N., 2013. Production of Turmeric Oleoresin Microcapsules by Complex Coacervation with Gelatin–Gum Arabic. J. Food Process Eng. 36, 364–373. https://doi.org/10.1111/jfpe.12003.